

An Affine moment invariant for multi-component shapes

Joviša Žunić¹, Miloš Stojmenović²

Abstract

We introduce an image based algorithmic tool for analyzing multi-component shapes here. Due to the generic concept of multi-component shapes, our method can be applied to the analysis of a wide spectrum of applications where real objects are analyzed based on their shapes - i.e. on their corresponded black and white images. The method allocates a number to a shape, herein called a multi-component shapes measure. This number/measure is invariant with respect to affine transformations and is established based on the theoretical frame developed in this paper. In addition, the method is easy to implement and is robust (e.g. with respect to noise).

We provide two small but illustrative examples related to aerial image analysis and galaxy image analysis. Also, we provide some synthetic examples for a better understanding of the measure behavior.

Keywords: Measuring shapes, multi-component shapes, pattern recognition, image processing.

¹Mathematical Institute, Serbian Academy of Sciences, Belgrade, Serbia
e-mail: jovisa_zunic@mi.sanu.ac.rs

²Department of Informatics and Computing, Singidunum University, Belgrade, Serbia
email: mstojmenovic@singidunum.ac.rs

1. Introduction

A shape is an object characteristic that can be described by several numerical characteristics. These numerical characteristics, herein called *shape measures*, are employed in many computer vision, image processing, and pattern recognition tasks [2, 4]. Shape measures are often designed to evaluate certain shape properties, like *elongation* [1, 25], *convexity* [14, 16], *tortuosity* [7], and many more. Some of these measures are generic, and aim to satisfy some specific properties such as rotational [8, 23] or affine [12, 5] invariance, for example. It is worth mentioning that a range of popular shape descriptors exist, and are extensively applied: algebraic [8], geometric [24], logical [19], fractal ones [10], and so on. In most cases the shape measures are combined and used together to achieve a better performance [3].

In this paper we define a measure applicable to multi-component shapes, which is invariant with respect to Affine transformations. We examine multi-component shapes in detail since they are not yet intensively studied in literature, whereas there exists a lot of the work related to Affine invariants, both in theory and practice.

1.1. Multi-component shapes

The concept of multi-component shapes has been presented in [27]. This is a very generic concept that allows us to segment a single object onto components, to group objects into a multi-component shape to suit a particular application. Some examples are given in Fig.1 and in the Experimental illustration section. Notice that some shape segmentation results can be natural (Fig.1(c)), while some can be more artificial (e.g. Fig.1(d,e)); some components can be connected, some not ((e.g. Fig.1(d,e))). Basically, there are no real restrictions on categorizing a shape as a being multi-component. Of

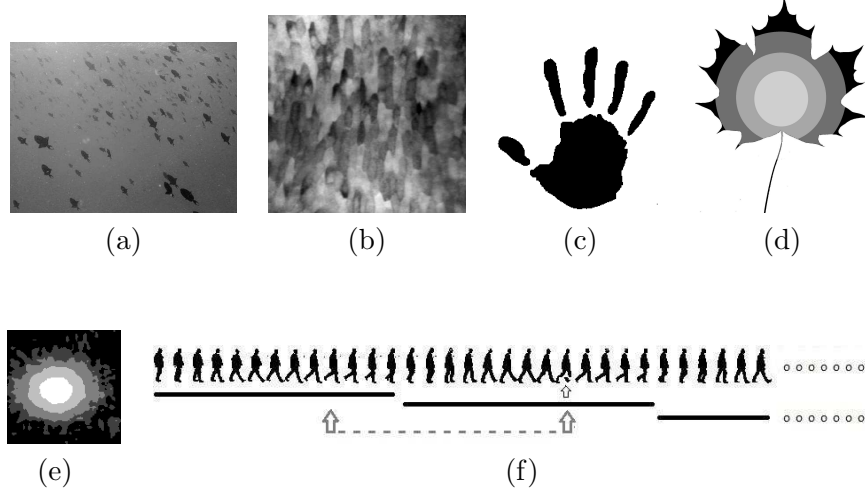


Figure 1: (a) School of Fish (b) Embryonic tissue with indistinct cell boundaries (c) Palm-print (d) leaf shape decomposed by concentric circles (e) galaxy shape obtained with a thresholding method [13] (f) Human gait – considered as a 13-component shape, whose components are the appearances of a walking person in a sequence of 13 consecutive frames.

course, a common requirement is that the selected segmentation well suits the desired application.

Examples (a) and (b), in Fig.1 are real images of a school of fish and an embryonic tissue, each of which have recognizable components. Their extracted components are in Fig.2. Shape (c) in Fig.1 represents a natural "decomposition" of a palm print while shapes (d) and (e), in the same figure represent an artificial or inaccurate decomposition of a leaf shape [15] and a galaxy shape, respectively, obtained using a thresholding method.

As expected, multi-component shapes are expected to have some properties that are not typical of single shapes. An example of such a property is the orientation of multi-component shapes. Indeed, in the case of relatively large numbers of components, it is expected that the orientation of a multi-component shape does not depend much on a "window" used for the

orientation computation [27, 17]. Two examples are found in Fig.2. The computed orientations of both halves, as well as the shape as a whole almost coincide for both (a) and (c) in Fig.2.

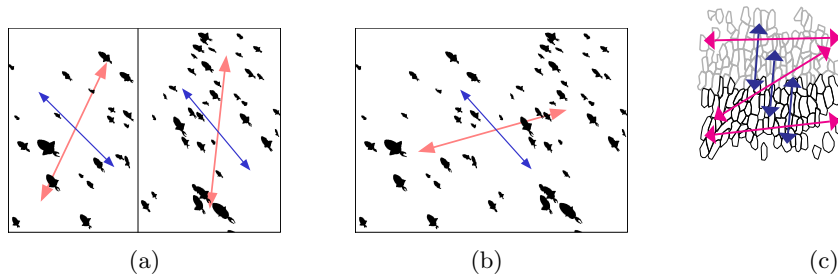


Figure 2: Orientations computed for (a) the separate left and right halves of the image, and also for (b) the complete image. The shorter dark blue arrows correspond to the shape orientations computed for the three sets of data according to our multi-component approach. In comparison, the long light red arrows correspond to the traditional method for computing orientation, in which each of the three sets of data are considered as representing single-component shapes (each containing multiple fish).

There already exist shape descriptors whose measures are only applicable for multiple component shapes. Some examples are anisotropy and disconnectedness of multi-component shapes [17, 28].

2. Preliminaries

Here we define the basic terms and introduce the notation used in this paper. We also give some well-known facts used for our derivations.

- The shape is a basic object property (like color or texture, for example). As such, shape does not need a formal definition. Shape is represented by a planar region, usually displayed as a binary (black-white) image.

- A multi-component shape $S = S_1 \cup S_2 \cup \dots \cup S_n$, having components S_1, S_2, \dots , and, S_n , is represented by n regions, corresponding to its components.

Note that the regions representing a component S_i do not need to be connected, in a topological sense.³ There is no formal restriction on how a given shape can be decomposed and presented as a multi-component shape. From a practical view-point such a decomposition should be meaningful in order to be beneficial for the desired application.

- Two shapes are considered equal if their set difference has an area equal to zero.

- The *geometric moment*, or simply *moment*, $m_{p,q}(S)$ of a given planar shape S is defined as

$$m_{p,q}(S) = \iint_S x^p y^q dx dy. \quad (1)$$

The moment $m_{p,q}(S)$ has the *order* equal to $p+q$. Obviously, $m_{0,0}(S)$, equals the area of S , while the moments $m_{1,0}(S)$ and $m_{0,1}(S)$ are used to define the *shape centroid*, denoted as $(x_c(S), y_c(S))$ and formally defined as

$$(x_c(S), y_c(S)) = \left(\frac{m_{1,0}(S)}{m_{0,0}(S)}, \frac{m_{0,1}(S)}{m_{0,0}(S)} \right). \quad (2)$$

- The normalized moments $\mu_{p,q}(S)$ are defined as

$$\mu_{p,q}(S) = \frac{1}{m_{0,0}(S)^{(p+q+2)/2}} \cdot \iint_S (x - x_c(S))^p (y - y_c(S))^q dx dy \quad (3)$$

³Formally, an n -component shape $S = S_1 \cup S_2 \cup \dots \cup S_n$, can be defined formally as a mapping $F((x, y))$: $S \rightarrow \{1, 2, \dots, n\}$. All of the points (x, y) with the same assigned value $F((x, y))$, belong to the same component, i.e. the k -th component S_k , where $1 \leq k \leq n$, is defined as $S_k = \{(x, y) \mid F((x, y)) = k\} = F^{-1}(k)$.

- Normalized moments $\mu_{p,q}(S)$ are translation and scaling invariant by definition. Both invariances are required in shape based tasks because shape properties do change under scaling and translation transformations.

- Many more moment invariants are used in shape based image analysis tasks. In his seminal work [8], Hu introduced seven quantities which are rotational invariants. Hu used algebraic reasoning, but later on Xu and Li [24] showed that Hu invariants are actually geometric invariants, and can be derived by considering certain geometric primitives defined by the shape points. Geometric reasoning will be applied here as well.

- Affine moment invariants are quantities computed from a set of moments that do not change under Affine transformation [5, 21]. The following Affine invariant will be exploited here

$$\mathcal{A}(S) = \mu_{2,0}(S) \cdot \mu_{0,2}(S) - \mu_{1,1}(S)^2. \quad (4)$$

- The Affine invariant $\mathcal{A}(S)$ has a simple geometric interpretation. Indeed, the squared area of the triangle whose vertices are points $(0,0)$, (x,y) , and (u,v) is

$$\frac{1}{4} \cdot (x \cdot v - y \cdot u)^2. \quad (5)$$

So, for a given shape S , having an area equal to 1, and all the triangles $\triangle ABC$ such that $A = (x,y) \in S$ and $B(u,v) \in S$ we easily obtain that a half of $\mathcal{A}(S)$ equals the total integral of the squared areas of triangles $\triangle ABC$:

$$\begin{aligned} & \iint_{(x,y) \in S} \iint_{(u,v) \in S} \frac{1}{4} \cdot (x \cdot v - y \cdot u)^2 dx dy du dv \\ &= \frac{1}{2} \cdot (\mu_{2,0}(S) \cdot \mu_{0,2}(S) - \mu_{1,1}(S)^2) = \frac{1}{2} \cdot \mathcal{A}(S). \end{aligned} \quad (6)$$

Such a simple geometric interpretation [29, 24] has been used in [29] to establish a shape interpretation of $\mathcal{P}(S)$. This interpretation of $\mathcal{P}(S)$ does not allow a simple extension to multi-component shapes. In the next section we will give a modified interpretation of $\mathcal{P}(S)$, which is extendable to multi-component shapes.

3. A new Affine invariant for multi-component shapes

As mentioned, we aim to develop a multi-component shape measure that is invariant with respect to Affine transformations. Our first idea was to exploit an existing Affine moment invariant $\mathcal{A}(S)$, as given in (6), defined for single-component shapes [5]. Such a measure has a nice geometric interpretation [24, 29] but is not easily extendable to measure multi-component shapes.⁴ So, we had to modify the equality in (6) and derive another geometric interpretation of the measure $\mathcal{A}(S)$. We show that $\mathcal{A}(S)$ (as given in (4)) equals the integral of the squared triangle areas, i.e. the integral of $Area_{\triangle}(\Delta ABC)^2$, where A , B , and C vary through a given shape S whose area is 1. We give the following theorem.

Theorem 1. *Let $A = (x, y)$, $B = (u, v)$, and $C = (z, \omega)$, be points belonging to a given shape S , having an area equal to 1,. The integral of all squared*

⁴To the best of our knowledge, this interpretation is novel, never before mentioned in literature. Since the idea is natural, it is still possible that it has been used and observed by others already.

areas of triangles ΔABC equals a quarter of $\mathcal{A}(S)$, or formally

$$\begin{aligned}
& \frac{1}{6} \iiint_{(x,y) \in S} \iint_{(u,v) \in S} \iint_{(z,\omega) \in S} (\text{Area_of_}\Delta ABC)^2 dx dy du dv dz d\omega \\
& \frac{1}{6} \cdot \iiint_{(x,y) \in S} \iint_{(u,v) \in S} \iint_{(z,\omega) \in S} \frac{1}{4} \cdot ((x-z)(v-\omega) - (y-\omega)(u-z))^2 dx dy du dv dz d\omega \\
& = \frac{1}{4} \cdot (\mu_{2,0}(S) \cdot \mu_{0,2}(S) - \mu_{1,1}(S)^2) = \frac{1}{4} \cdot \mathcal{A}(S). \tag{7}
\end{aligned}$$

Proof. We do not give a complete proof here. Even though the derivation might be seen as a long and messy one, it is still trivial. Here are some hints to support the derivations.

- The formula in (5) for the points $(x-z, y-\omega)$, $(u-z, v-\omega)$, and $(z-z, \omega-\omega) = (0, 0)$, should be used.
- The identity $\iiint_{(x,y) \in S} \iint_{(u,v) \in S} \iint_{(z,\omega) \in S} x^a y^b u^c v^d z^e \omega^f dx dy du dv dz d\omega = \mu_{a,b}(S) \cdot \mu_{c,d}(S) \cdot \mu_{e,f}(S)$ should be applied.
- The factor $\frac{1}{6}$ comes from the fact that three points (x, y) , (u, v) , and (z, ω) , determine the same triangle, independently on order they have been selected. ■

Now, we have the idea and necessary theoretical framework regarding how to define the affine moment invariant for multi-component shapes. Briefly, we observe all points that do not belong to a single shape component and the integral of the squared areas of the triangles determined by these points. Rather than manipulate with all three points (i.e. observed triangle vertices) that do not belong to the same component, we observe the squared triangle areas determined by all of the triplets of points that do belong to the n-component shape $S = S_1 \cup S_2 \cup \dots \cup S_n$ and take the areas of all the

triangles whose vertices belong to the same component. This is just for the sake of a simpler computation.

Since the shape S and all of the components of S should play a role in the computation of its new Affine invariant measure, the size of all of these appearing shapes should be taken into account. We have the following identity (see (3)), for the shapes whose area is not equal to 1:

$$\begin{aligned} m_{2,0}(S) \cdot m_{0,2}(S) - m_{1,1}(S)^2 &= \\ \mu_{0,0}(S)^4 \cdot (\mu_{2,0}(S) \cdot \mu_{0,2}(S) - \mu_{1,1}(S)^2) &= \mu_{0,0}(S)^4 \cdot \mathcal{A}(S). \end{aligned} \quad (8)$$

As mentioned, we observe the integral of squared areas of all triangles whose vertices do belong to the same component of the n -component shape S from the integral of squared areas of all triangles whose vertices belong to the shapes S . This quantity can be computed as

$$(m_{2,0}(S) \cdot m_{0,2}(S) - m_{1,1}(S)^2) - \sum_{i=1}^{i=n} (m_{2,0}(S_i) \cdot m_{0,2}(S_i) - m_{1,1}(S_i)^2) \quad (9)$$

or equivalently in the following form

$$\begin{aligned} m_{0,0}(S_1 \cup \dots \cup S_n)^4 \cdot (\mu_{2,0}(S) \cdot \mu_{0,2}(S) - \mu_{1,1}(S)^2) \\ - \sum_{i=1}^{i=n} m_{0,0}(S_i)^4 \cdot (\mu_{2,0}(S_i) \cdot \mu_{0,2}(S_i) - \mu_{1,1}(S_i)^2). \end{aligned} \quad (10)$$

If we normalize the above form, i.e. divide both summands with $(m_{0,0}(S_1 \cup \dots \cup S_n))^4$ we get the quantity

$$\mathcal{A}(S_1 \cup \dots \cup S_n) - \frac{1}{m_{0,0}(S_1 \cup \dots \cup S_n)^4} \cdot \sum_{i=1}^{i=n} m_{0,0}(S_i)^4 \cdot \mathcal{A}(S_i). \quad (11)$$

that will be used to define a new Affine measure $\mathcal{M}(S)$ for multi-component shapes. We give the following definition.

Definition 1. *Let an n -component shape S be given. We define the multi-component shape measure $\mathcal{M}(S)$, for such a shape S , by the following equality*

$$\begin{aligned} \mathcal{M}(S) &= \mathcal{M}(S_1 \cup \dots \cup S_n) \\ &= \mathcal{A}(S_1 \cup \dots \cup S_n) - \frac{1}{m_{0,0}(S_1 \cup \dots \cup S_n)^4} \cdot \sum_{i=1}^{i=n} m_{0,0}(S_i)^4 \cdot \mathcal{A}(S_i) \end{aligned} \quad (12)$$

4. Experimental Illustrations

Several experimental illustration are given in this section in order to enable an easier understanding of the behavior of the new measure $\mathcal{M}(S)$.

First experiment. In this experiment we illustrate the diversities in representing a shape as being multi-component. We use a hand shape, displayed in Fig.3(a). In the first instance, the shape in Fig.3(a) can be treated as a 6-component shape, whose components are the palm and five fingers, each taken as a separate component. In such a case the computed measure value is $\mathcal{M}_{6-comp.}(S) = 0.0109$.

The hand shape in Fig.3(a) can also be observed as a 2-component shape. It is possible to select the palm (as displayed in Fig.3(b)) as one component and all five fingers as the other component (S displayed in Fig.3(c)). In this case the computed measure is $\mathcal{M}_{2-comp.}(S) = 0.0177$.

To complete this discussion, it is worth mentioning that if the palm is considered as a 1-component shape, then $\mathcal{M}_{1-comp.}(S) = 0$, which is in accordance with the Definition 1, i.e. the computed measure $\mathcal{M}_{1-comp.}(S)$ of all 1-component shapes is equal to zero. If the shape consists of five fingers,

as displayed in Fig.3(c), then the computed measure is $\mathcal{M}_{5-comp.}(S) = 0.1972$.

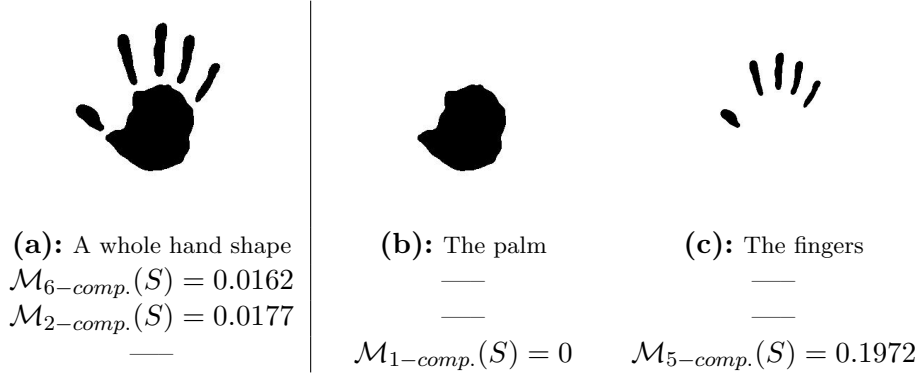


Figure 3: The shape on the left is treated as being 2-component (five fingers as one components and the palm as the second component) and its computed measure is $\mathcal{M}_{2-comp.}(S) = 0.0177$. Treating the same shape as being 6-component (five fingers, each a separate component, and the palm, as the final component), the computed measure is $\mathcal{M}_{6-comp.}(S) = 0.0162$. The measure values for the 1-component shape and the 5-component shape in Fig.3(b)&(c) are 0 and 0.1972, respectively.

Second experiment. In this experiment we illustrate that $\mathcal{M}(S)$ depends on the distances between shape components. Precisely, as such distances increase, the $\mathcal{M}(S)$ values increase as well. In each sub-figure in Fig.4, there are four identical squares, but with varying distances between each other. As the distance between these squares increases, the measured values $\mathcal{M}(S)$ increase as well. Notice that this is in accordance with the definition of $\mathcal{M}(S)$.

Third experiment. An aerial image (Cardiff, U.K.) is in Fig.5, on the right. The extracted edges of the buildings are in the image in the middle. The obtained edges are skewed such that the rectilinearity measure (for detail see [18]) of the building contours is maximized. The obtained values for the two 5-component shapes are almost identical ($\mathcal{M}(middle-image) =$

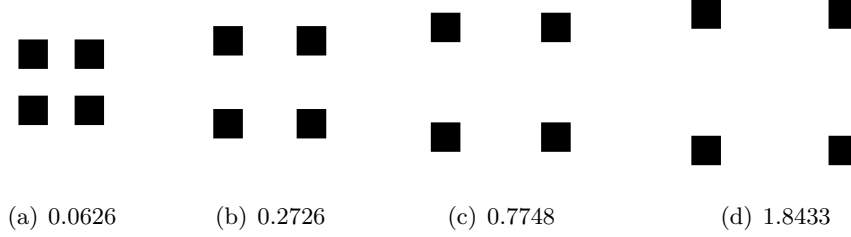


Figure 4: 4-component shapes and their assigned $\mathcal{M}_{4-comp.}(S)$ values (given below each shape)

0.0324 and $\mathcal{M}(\text{image} - \text{on} - \text{the} - \text{right}))$, as expected. There is a small difference caused by the numerical calculation.

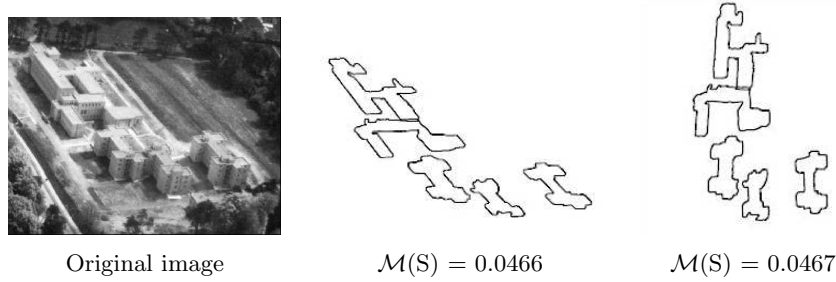


Figure 5: The images are taken from [18]: The original aerial image is on the left. The extracted contours (from the original images) are in the middle. The skewed contours, such that the rectilinearity measure is maximized, are on the right.

Fourth experiment. In this experiment we illustrate the potential of the new measure to be used in a galaxy shape analysis task. Elliptical and spiral galaxies, listed in the popular Nearby Galaxy Catalog [6], are selected to illustrate a discriminative capacity of $\mathcal{M}_{3-comp.}(S)$. The results for spiral galaxies are in Fig.6, while the results for elliptical galaxies are in Fig.7. The original galaxy images are on the left, in each row, in both Fig.6 and Fig.7. A median filter has been applied to these original images. The filtered images are in the second column, in both related images. Multi-components of the

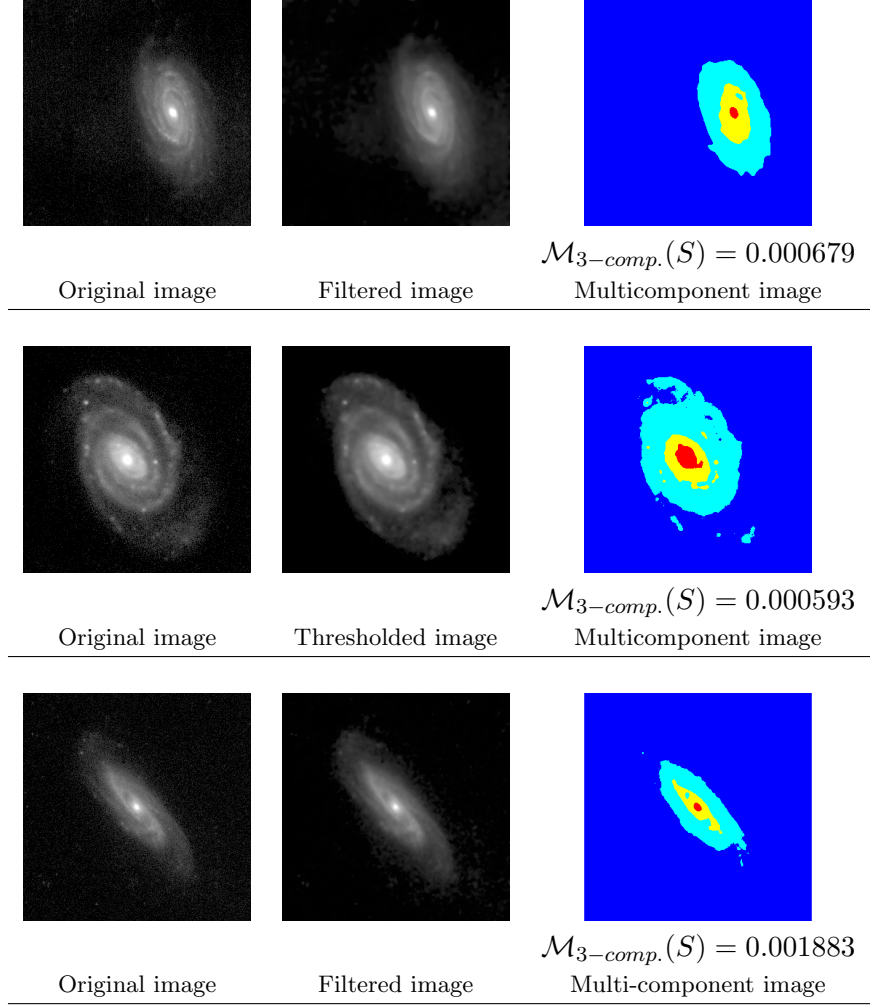


Figure 6: The original images of the three spiral galaxies, from [6], are displayed on the left, in each row. The images in the second column, are obtained by applying a median filter, to the original galaxy images. The images on the right are 4-component images, obtained by a thresholding method. Three components are used for the $\mathcal{M}_{3-comp}(S)$ computation, while the fourth component corresponds to the galaxy background.

filtered images are obtained by applying a multi threshold method. These images are on the right. Four components were obtained for each galaxy filtered image. Three of them are used as galaxy image components, and

the fourth component corresponds to the galaxy background. The computed $\mathcal{M}_{3-comp.}(S)$ measure is immediately below the thresholded images. The

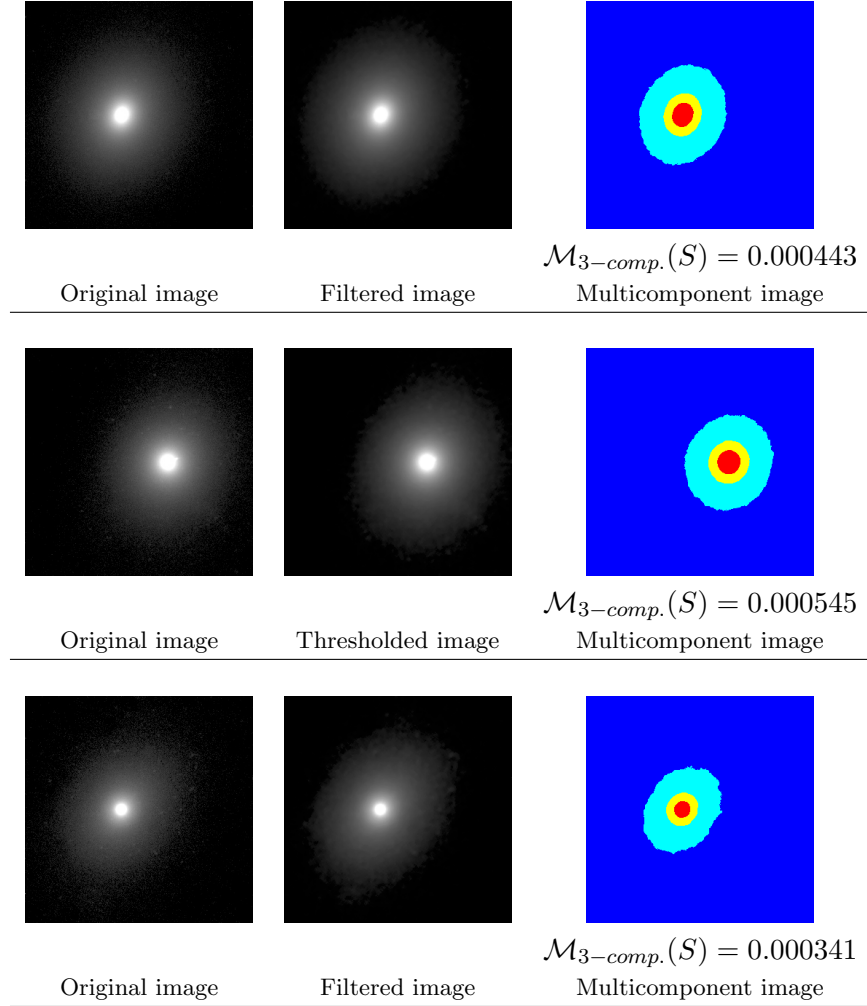


Figure 7: The original images of the three elliptical galaxies, from [6], are displayed on the left, in each row. The images in the second column, are obtained by applying a median filter, to the original images. The images on the right are 4-component shapes, obtained by a thresholding method. Three components are used for the $\mathcal{M}_{3-comp.}(S)$ computation, while the fourth component corresponds to the galaxy background.

measure $\mathcal{M}_{3-comp.}(S)$ distinguishes between spiral and elliptical galaxies

very well. The values for $\mathcal{M}_{3-comp.}(S)$ are 0.000679 (for the galaxy image in the first row), 0.000593 for the galaxy image in the second row, and 0.001883 for the galaxy image in the third row (see Fig.6). The computed $\mathcal{M}_{3-comp.}(S)$ values are smaller for the three selected elliptical galaxies. They are 0.000545, 0.000341, and 0.000341, respectively.

5. Conclusion

A new shape measure $\mathcal{M}(S)$ has been introduced. The new measure is Affine invariant and is designed to be applicable to multi-component shapes. The measure is developed by exploiting a new geometric interpretation of the well-known Affine invariant [5]: $\mathcal{A}(S) = \mu_{2,0}(S) \cdot \mu_{0,2}(S) - \mu_{1,1}(S)^2$ (see (4)). This new interpretation of $\mathcal{A}(S)$ says that $\mathcal{A}(S)$ is proportional to the total integral of the squared areas of all the triangles whose vertices belong to S . Another interpretation of $\mathcal{A}(S)$ can be found in [24], but this interpretation does not allow an easy application to the multi-components shapes measurement. The new interpretation of $\mathcal{A}(S)$ enables an easy and natural extension of $\mathcal{A}(S)$ to multi-component shapes. As such, the new measure $\mathcal{M}(S)$ is very flexible, because the concept of multi-component shapes is very generic. Indeed, a given shape can be decomposed into components in various ways. Also, the number of components can be selected in different ways. All this has been illustrated on illustrative experimental examples.

The new measure $\mathcal{M}(S)$ is an Affine invariant. The suitability of the Affine invariance property for multi-component shape analysis is also illustrated. The task of matching aerial photos of objects on the ground (please see the third experiment) was given as an illustration.

Being an area based measure, i.e. a measure that uses all of the shape points for its computation, it is efficient to compute [9, 11]. This is not a

case for boundary based shape measures, e.g. [17, 20, 25].

References

References

- [1] M. A. Aktas, J. Žunić: A family of shape ellipticity measures for galaxy classification. *SIAM Journal on Imaging Sciences*, **6**:765–782, 2013.
- [2] F. Cao, J.-L. Lisani, J.-M. Morel, P. Musé, F. Sur. A theory of shape identification, Springer, 2008.
- [3] J. B. de Carvalho, G.J.A. do Amaral: Classification methods for planar shapes. *Expert Systems with Applications*, **151** paper 113320, 2020.
- [4] L. d. F. Costa, R. M. Cesar Jr.: Shape classification and analysis: theory and practice, CRC Press, 2009.
- [5] J. Flusser and T. Suk: Pattern recognition by Affine moment invariants. *Pattern Recognition*, **26**:167–174, 1993.
- [6] Z. Frei, P. Guhathakurta, J. E. Gunn, and J. A. Tyson: A catalog of digital images of 113 nearby galaxies. *Astronom. J.*, **111**:174–181, 1996.
- [7] E. Grisan, M. Foracchia, A. Ruggeri: A novel method for the automatic grading of retinal vessel tortuosity. *IEEE Transactions on Medical Images*, **27**:310–319, 2008.
- [8] M. K. Hu: Visual pattern recognition by moment invariants. *IRE Transactions on Information Theory*, **8**:179–187, 1962.
- [9] M.N. Huxley, R. Klette, J. Žunić: ‘Precision of geometric moments in picture analysis,’ chapter in Geometric Properties from Incomplete

- Data, editors: R. Klette, R. Kozera, L. Noakes, J. Weickert, pp. 221-235, Springer, 2006.
- [10] A. R. Imre: Fractal dimension of time-indexed paths, *Applied Mathematics and Computation*, **207**:221–229, 2009.
 - [11] R. Klette, J. Žunić: Multigrid Convergence of Calculated Features in Image Analysis, *J. Math. Imaging Vis.*, **13**:173-191, 2000.
 - [12] Y. Mei, D. Androutsos: Robust affine invariant region-based shape descriptors: The ICA Zernike moment shape descriptor and the whitening Zernike moment shape descriptor, *IEEE Signal Processing Letters*, **16**:877-880, 2009.
 - [13] N. Otsu: A threshold selection method from gray-level histograms. *IEEE Transactions on Systems, Man, and Cybernetics*, **9**:62–66, 1979.
 - [14] E. Rahtu, M. Salo, J. Heikkilä: A new convexity measure based on a probabilistic interpretation of images. *IEEE T. Pattern Analysis Mach. Intell.* **28**:1501–1512, 2006.
 - [15] M. B. H. Rhouma, J. Žunić, M. C. Younis: Moment invariants for multi-component shapes with applications to leaf classification. *Computers and Electronics in Agriculture*, **142**:326–337, 2017.
 - [16] P. L. Rosin, C. L. Mumford: A symmetric convexity measure. *Computer Vision and Image Understanding*, **103**:101–111, 2006.
 - [17] P. L. Rosin, J. Žunić: Orientation and anisotropy of multi-component shapes from boundary information. *Pattern Recognit.*, **44**: 2147–2160, 2011.

- [18] P. L. Rosin, J. Žunić: Measuring rectilinearity. *Comput. Vis. Image Underst.*, **99**:175–188, 2005.
- [19] H. Schweitzer, J. Straach: Utilizing moment invariants and Gröbner bases to reason about shapes, *Computational Intelligence*, **14**:461–474, 1998.
- [20] M. Stojmenović, J. Žunić: Measuring Elongation from Shape Boundary. *J. Math. Imaging Vis.*, **30**:73–85, 2008.
- [21] T. Suk and J. Flusser: Affine moment invariants generated by graph method. *Pattern Recognition*, **44**:2047–2056, 2011.
- [22] A. Q. Tool: A method for measuring ellipticity and the determination of optical constants of metals. *Physical Review (Series I)*, **31**:1–25, 1910
- [23] B. Wang: Shape retrieval using combined Fourier features. *Optics Communications*, **284**:3504–3508, 2011.
- [24] D. Xu, H. Li: Geometric moment invariants. *Pattern Recognition*, **41**:240–249, 2008.
- [25] A. Žunić: Shape diameter for object analysis. *Inf. Procc. Letters*, **136**:76–79, 2018.
- [26] J. Žunić, P. L. Rosin: Rectilinearity measurements for polygons. *IEEE Trans. Pattern Anal. Mach. Intell.*, **25**:1193–1200, 2003.
- [27] J. Žunić, P. L. Rosin: An Alternative Approach to Computing Shape Orientation with an Application to Compound Shapes. *Int. J. Comput. Vis.*, **81**: 138–154, 2009.

- [28] J. Žunić, P. L. Rosin, V. Ilić: Disconnectedness: A new moment invariant for multi-component shapes. *Pattern Recognition*, **78**:91–102, 2018.
- [29] J. Žunić, D. Žunić: Shape interpretation of second moment invariants. *Journal of Mathematical Imaging and Vision*, **56**:125–136, 2016.